19th Australasian Fluid Mechanics Conference
Melbourne, Australia
8-11 December 2014

Effect of a Sinusoidal Leading Edge Pattern on Flat Plate Boundary Layer Flow

S.M. Hasheminejad[1], H. Mitsudharmadi[2] and S.H. Winoto[1]

[1] Department of Mechanical Engineering
National University of Singapore, 9 Engineering Drive 1, Singapore117575, Singapore

[2]Temasek Laboratories

National University of Singapore, T-Lab Building, 5A, Engineering Drive 1, Singapore117411, Singapore

Abstract

Aerofoils with a sinusoidal leading edge pattern have been the subject of the study during the recent decade due to its considerable effect on the aerodynamics performance. The leading edge variation results in the formation of streamwise counter-rotating vortices which affect the boundary layer development on aerofoils. To understand the influence of the leading edge variation to the boundary layer flow development, the current study was carried out using a flat plate model. A single hot-wire anemometer was used to measure the streamwise velocity at Reynolds number (based on the wavelength of the leading edge patterns) of 3080 corresponding to free-stream velocity of 3 m/s. The results showed that downstream of the troughs of the leading edge pattern, counter- rotating pairs of vortices form and develop along the streamwise direction. Inflection points on the velocity profiles at upwash region imply the appearance of the vortices with mushroom like structure which diffuse further downstream as a consequence of the mixing enhancement and eventually break down into turbulence.

Introduction

Use of Geometrical patterns on the leading edge of a flat plate will result in the generation of the streamwise counter-rotating vortices in its boundary layer. If an aerofoil is used instead, its aerodynamic performance will be improved through enhancement and/or reduction of lift and drag forces. Separation delay is also another result which likely happens due to the appearance of the stream-wise vortices. The idea of the leading edge pattern was actually inspired by nature. For example, observations showed that vortices generated by the comb like feathers of owl wings enable this bird to silently approach the prey by a high stall angle of attack. Actually, the feathers causes the boundary layer separation to be retarded [1]. In another example, biologists observed that the humpback whale (Megaptera novaeangliae) is more manoeuvrable compared with other species of whales in pursuing the prey even though it has a huge inflexible body. Such behaviour is attributed to the combination of sinusoidal tubercles and the high aspect ratio of the flippers which leads to a rise in proportion of lift to drag coefficients. This change in lift to drag ratio allows this marine mammal perform sharp banking turns [4, 5]. Soderman [13] studied the effect of the saw-tooth edge attached to the leading edge of a two-dimensional aerofoil. The results showed that the saw-tooth pattern leading edge can reduce the separation region and drag coefficient. A series of wind tunnel experiments by Miklosovic et al. [11] showed increase of the stall angle and the maximum lift coefficient by 40% and 6%, respectively. They also found that unlike regular aerofoils, the lift gradually drops during the stall. Stein and Murray [14] examined a two-dimensional aerofoil with the same amplitude and wavelength as the humpback whale flipper. Unlike in previous works, they reported a considerable loss of lift and an increase in drag for a specific range of angles of attack [14]. This discrepancy in results may be due to the fact that the earlier work was done on finite aerofoils. This also indicates that the spanwise flow has been affected by the leading edge protuberances. Johari et al. [9] experimentally studied the role of sinusoidal protuberances on the leading edge of a two-dimensional aerofoil and observed that the amplitude of the protuberances plays a more significant role on the performance than their wavelength. They also found from flow visualization that the flow separation occurs earlier in the region between two protuberances [9]. Force measurement tests [6, 9, 10, 14] at low Reynolds number on nominally two-dimensional aerofoils demonstrated gradual stall with greater post stall lift for the modified model compared to the unmodified one. However, the pre stall performance for both modified and unmodified models was more or less the same. It can be concluded that the tubercles have limitation to be used in bounded aerofoils, that is, for cases which can be considered as infinite two-dimensional aerofoils [3, 9, 10, 15]. Cranston et al. [3] used leading edge serrations (saw-tooth like pattern) on flat plates and showed that the size of the serrations for low Reynolds number flow affects the aerodynamics characteristics and bubble separation. They found that the use of the serrations is more efficient at higher Reynolds numbers. The use of small serrations lead to increase in lift coefficient, while the large serrations result in a reduction in lift. Hansen et al. [6] studied two different aerofoils NACA 0021 and NACA 65-021, to find the effect of aerofoil shape characteristics on improvement of the aerodynamic performance. They found that shifting the position of the maximum thickness further downstream extends the laminar boundary layer further and make the tubercles effect more noticeable. They confirmed that as the amplitude of tubercles decreased the aerodynamic performance decreased too. In contrast to earlier researches by [9, 15], they reported that both amplitude and wavelength have considerable effect. They also showed that there is a critical wavelength at which the performance is maximum for each amplitude. Therefore, they defined an optimal amplitude-to-wave- length ratio for which the best performance would be achievable [6]. Weber et al. [16] used tubercles on the leading edge of rudder and found that the tubercles enhance lift at high angles of attack, as well as cause a more favourable control during turning. Using leading edge protuberances on the blades of industrial fans by a Canadian company reportedly resulted in improvement in efficiency, electricity consumption and noise level [12]. The use of tubercles technology in power generation through renewable resources has also shown its effectiveness. For example, a 35 kW wind turbine which utilized tubercles technology on its blades has been introduced and tested. The test results showed that this design produced more electricity at moderate wind speeds [8]. Chen et al. [2] carried out an experimental study on delta wings with low swept angle fitted with various sinusoidal leading edges. Although the results showed almost no change in lift-to-drag ratio, the stall is delayed with no penalty on the maximum lift coefficient. This fact would be very significant for manoeuvrability and agility of aircrafts using swept

wings. Recently, Hasheminejad et al. [7] performed some visualization experiments to find the influence of different geometrical patterns on a flat plate leading edge. However, the mechanism of the leading edge pattern on the flow structures generated is not well understood yet. However, the mechanism of the leading edge pattern on the flow structures generated is not well understood yet.

The objective of this work is to study the vortex structure and laminar- turbulence transition process in the boundary layer of flat plate with sinusoidal leading edge pattern. For this purpose, hot-wire anemometry measurement was performed to examine the effect of the sinusoidal leading edge on the boundary layer flow.

Experimental Details

The experiments were conducted in a 235cm straight plexiglass duct with rectangular cross-section of 150 mm×600 mm. The rectangular duct is connected to a low speed, blow down type wind tunnel shown in figure 1. A fan at upstream end generated the required flow for experiments. A honeycomb and five rectangular fine- mesh screens with the coarser mesh size positioned upstream were used in settling chamber to control the flow. Downstream of the finest mesh screen placed at the end of the settling and prior to the experiment duct, a contraction chamber was installed. The chamber is made of a 300mm straight channel with 600mm×600mm cross section. The chamber is connected to the experiment duct by a two- dimensional contraction cone as a cross-section reducer. The turbulence intensity of free stream velocity within the test section is less than 0.45% for the velocity range of U_∞=1.0- 4.0 m/s.

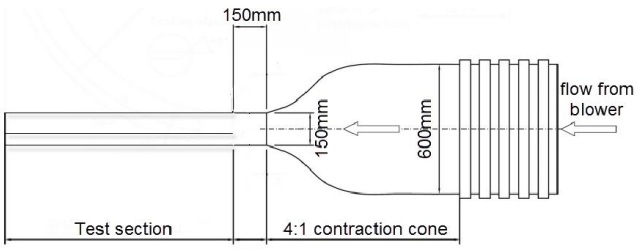

Figure 1. Schematic of experimental setup

A flat plate of 3mm thickness is mounted inside the channel while the distance from the top and the bottom surfaces of the channel are 100mm and 50mm respectively. To avoid bubble separation, the leading edge of the flat plate was made sharp by machining with acute angle of 20°. As shown in figure 2, the flat plate has a rectangular cut with cross section of 150mm ×240mm which is completed by a flat plate with sinusoidal leading edge pattern as the test plate. The thickness and the leading edge slope of the test plate are as same as those of the main plate. The test plate is supported by 3 pieces of 1 mm thick plates from the bottom side attached to the main plate to keep it aligned with the main plate. The sinusoidal pattern consists of a sinusoid with eight cycles defined by wavelength and amplitude of 15 mm and 7.5mm, respectively. Figure 2 shows the configuration and the details of the test plate. To measure the streamwise mean and fluctuating velocity, a single hot wire probe specially designed for boundary layer measurement (DANTEC 55p15) was used for the present study. The probe functioned in a Constant Temperature Anemometer mode was traversed in the spanwise and normal directions at several streamwise locations to collect the streamwise velocity data. The output of CTA was coupled to an analog filter in order to low pass filter the signal at 3KHz and sampled at 6KHz for 21 seconds. An analog to digital convertor board connected to a personal computer was employed to digitize the collected data. Eventually, the data were analysed and prepared for post processing using HPVEE software.

A Pitot- static tube was placed above the hot-wire probe at the free stream velocity region. The Pitot- static tube was linked to a pressure transducer which was calibrated against a micro-manometer. The Pitot- static tube use was used for hot- wire calibration and the local free- stream velocity monitoring before and during the experiments respectively.

Measurement on the y-z plane were done with step size of 1.0 mm in the spanwise direction (z) and 0.1 -1 mm in the normal direction (y). To have an accurate movement along spanwise and normal direction, a traversing mechanism was used while the hot- wire and the Pitot- static tube mounted on. The movement of the traversing mechanism was controlled by two identical step motors with accuracy of ±0.01 mm along y- and z-direction.

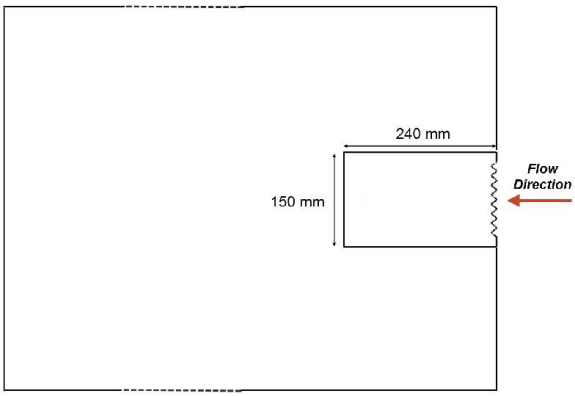

Figure 2. Schematic of the test plate configuration.

Results and Discussion

Data were collected at some streamwise positions (x) from the flat plate leading edge at Reynolds number (based on the wavelength of leading edge patterns) of 3080 which corresponds to the flow velocity of 3 m/s. Inasmuch as the characteristics of vortices are very similar, measurement was only performed for the two middle trough of the pattern. The results showed that streamwise vortices within the boundary layer for the present study is qualitatively in good agreement with what is previously reported by Hasheminejad et al. [16]. They conducted smoke visualization experiment on a triangular and semicircular leading edge with the same amplitude and wavelength as the present investigation. As observed, immediately downstream of every trough of the sinusoidal pattern, boundary layer is changed three-dimensionally due to formation of counter- rotating pairs of vortices. The development of streamwise vortices in the boundary layers is initiated by immediate mushroom structures followed by decay of them prior to turbulence. In fact, leading edge variation changes streamwise momentum distribution which causes spanwise variation in the boundary layer thickness. Downstream of the troughs is known as upwash region where low momentum fluid moves away from surface and make the boundary layer thicker. While downstream of the pattern peaks, outer high momentum fluid moves toward the surface and form downwash region. Figure 3 shows spanwise distribution of normalized streamwise velocity on y-z plane at different $\eta=y/\delta$ (where δ is the Blasius boundary- layer thickness) for some streamwise (x) locations. As can be seen, at upwash the fluid has lower momentum than downwash. In fact, the low momentum fluid is lifted up but cannot enter the free stream with higher momentum. Deflected flow returns down toward the surface and causes the high momentum fluid to be entrained in downwash region. Such fluid movement leads to formation of a pair of counter rotating vortices with mushroom-like structure.

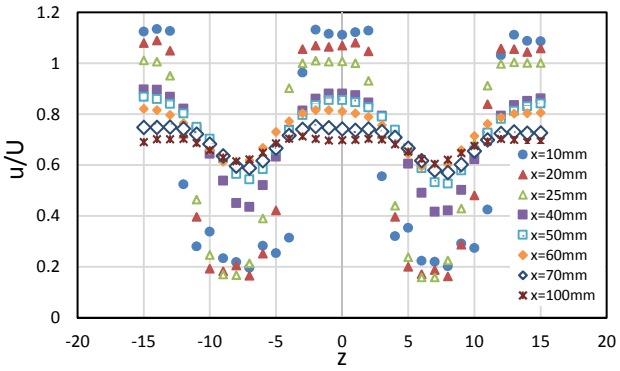

(a) at η=2.5

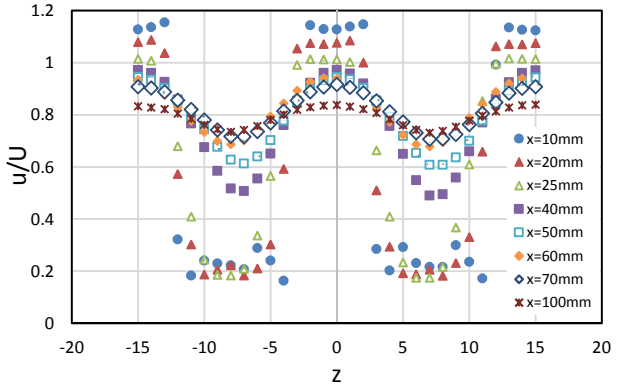

(b) at η=5

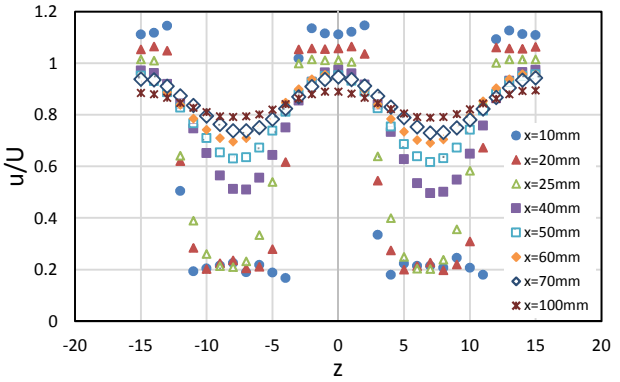

(c) at η=7.5

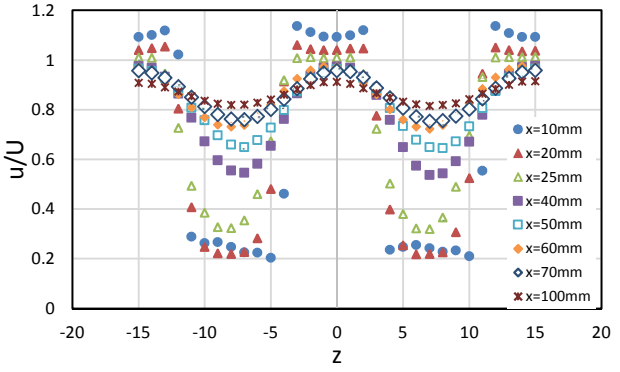

(c) at η=10

Figure 3. Spanwise distributions of normalized velocity at different normal and streamwise locations.

Regarding the considerable variation in spanwise distribution velocity, appearance of the streamwise vortices occurs immediately after each trough (figure 3). The vortices continuously grow with mushroom-like shape till x ≈ 30 mm. Then, they start to decay while the mushroom structure are still maintained. From location x ≈ 80 mm onward, small change in velocity particularly at upwash indicates that the vortices growth is being halted. Furthermore, the spanwise variation becomes flattened as a result of mixing enhancement and consequently, the mushroom-like structure is diffused. The streamwise velocity normal to the surface at upwash and downwash regions for several locations is represented in figure 4. As shown, the velocity profiles have inflection points.

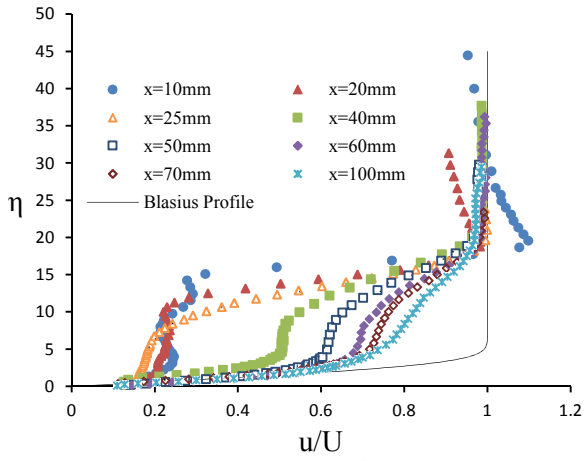

(a) at upwash

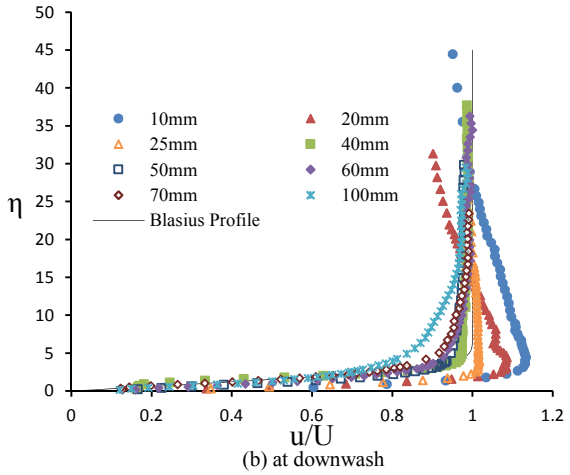

(b) at downwash

Figure 4. Streamwise velocity profiles normal to the surface at some streamwise (x) locations.

As can be seen, the velocity profile at x=10 mm has two inflection points indicating strong upwash which becomes one point at further downstream velocity profiles. At location x=100mm there is almost no trace of the inflection due to diffusion of the mushroom-like vortices. Moreover, further downstream of location x=10mm, the profiles initially become thinner but after location x=25mm become fuller. In contrast, no inflection point finds on the velocity profiles at downwash. At downwash, the velocity profiles are fuller than those at upwash. Additionally, near the leading edge (x=10,20mm), the streamwise velocity around the and between vortices exceeds the freestream velocity. It happens because of the entrainment of the high momentum fluid at downwash.

Conclusions

Based on the obtained data from hot- wire velocity measurement, the flow fields over a flat plate induced by sinusoidal leading edge. The sinusoidal pattern consists of a sinusoid with eight cycles defined by wavelength and amplitude of 15 mm and 7.5mm, respectively. The spanwise distribution of the normalized velocity on y-z plane at different normal wall positions for some streamwise locations revealed that downstream of the pattern trough, the momentum is altered and consequently counter-rotating pairs of vortices are generated which change the boundary layer. These streamwise vortices develop in the boundary layer with mushroom- like structures and break down into turbulence further downstream. Although the decay process of the vortices is triggered at location x=30 mm, they retain the mushroom-like structure prior to breakdown into turbulence at x≈80 mm.

Plotting velocity profiles showed that, at upwash region, there are inflection points on the profiles due to appearance of the vortices with mushroom-like structure. The profile inflection gradually disappear further downstream as the vortices breakdown into turbulence. However, the velocity profiles do not experience any inflection point.

References

[1] Anderson, G. W., An Experimental Investigation of a High Lift Device on the Owl Wing, Air force Institute of Technology, Wright-Patterson AFB, School of Engineering, Ohio, United States, 1973.

[2] Chen, H., Pan, C. & Wang, J., Effects of Sinusoidal Leading Edge on Delta Wing Performance and Mechanism, *Science China Technological Sciences*, Vol. 56, No. 3, 2013, pp. 772-779.

[3] Cranston, B., Laux, C. & Altman, A., Leading Edge Serrations on Flat Plates at Low Reynolds Number, in 50*th AIAA Aerospace Sciences Meeting Including the New Horizons Forum and Aerospace Exposition*, Nashville, 2012.

[4] Fish, F. E. & Battle, J. M., Hydrodynamic Design of the Humpback Whale Flipper, *Journal of Morphology*, Vol. 225, No. 1, 1995, 51-60.

[5] Fish, F. E., Weber, P. W., Murray, M. M. & Howle, L. E., The Tubercles on Humpback Whales' Flippers: Application of Bio-Inspired Technology, *Integrative and Comparative Biology*, Vol. 51, No. 1, 2011, 203-213.

[6] Hansen, K. L., Kelso, R. M. & Dally, B. B., Performance Variations of Leading-Edge Tubercles for Distinct Airfoil Profiles, *AIAA Journal*, Vol. 49, No. 1, 2011, 185- 194.

[7] Hasheminejad, S. M., Mitsudharmadi, H.& Winoto, S. H., Effect of Flat Plate Leading Edge Pattern on Structure of Streamwise Vortices Generated in Its Boundary Layer. *Journal of Flow Control, Measurement & Visualization*, 2014, Vol. 2, No. 1,18-23.

[8] HOWLE, L. E., A Report in the Efficiency of a Whale Power Corp. 5 Meter Prototype Wind Turbine Blade, Whale power Wenvor Blade, BelleQuant, LLC, Durham, 2009.

[9] Johari, H., Henoch, C. W., Custodio, D. & Levshin, A., Effects of Leading-Edge Protuberances on Airfoil Performance, *AIAA Journal*, Vol. 45, No. 11, 2007, 2634-2642.

[10] Miklosovic, D. S., Murray, M. M. & Howle, L. E., Experimental Evaluation of Sinusoidal Leading Edges, *Journal of Aircraft*, Vol. 44, No. 4, 2007, 1404-1408.

[11] Miklosovic, D. S., Murray, M. M., Howle, L. E. & Fish, F. E., Leading-Edge Tubercles Delay Stall on Humpback Whale (*Megaptera novaeangliae*) Flippers, *Physics of Fluids*, Vol. 16, No. 5, 2004, 39.

[12] Ontario Power Authority, "Energy Efficient Fans Take Their Cue from the Humpback Whale," 2010. http://archivepowerauthority.on.ca/Storage/122/16957_AgNews_July231.pdf

[13] Soderman, P. T., Aerodynamic Effects of Leading-Edge Serrations on a Two-Dimensional Airfoil, *NASA TM X-2643* United States, 1972, 39.

[14] Stein, B. & Murray, M., Stall Mechanism Analysis of Humpback Whale Flipper Models, *Proceedings of Unmanned Untethered Submersible Technology* (*UUST*), *UUST*05, 2005, 5.

[15] Van Nierop, E. A., Alben, S. & Brenner, M. P., How Bumps on Whale Flippers Delay Stall: An Aerodynamic Model, *Physical Review Letters*, Vol. 100, No. 5, 2008, 054502.

[16] Weber, P. W., Howle, L. E. & Murray, M. M., Lift, Drag, and Cavitation Onset on Rudders with Leading-Edge Tubercles, *Marine Technology*, Vol. 47, No. 1, 2010, 27-36.